



CrossMark
click for updates

Cite this: *RSC Adv.*, 2016, 6, 112175

Multispectroscopic analysis and molecular modeling to investigate the binding of beta lactoglobulin with curcumin derivatives†

Sanhita Maity, Sampa Pal, Subrata Sardar, Nayim Sepay, Hasan Parvej, Jishnu Chakraborty and Umesh Chandra Halder*

Bovine beta lactoglobulin (β -lg), the major whey protein, has a great affinity for a wide range of organic compounds like fatty acids, retinol etc. Curcumin, a polyphenolic antioxidant present in turmeric and its isoxazole (IOC) and pyrazole (PY) derivatives have been elicited worldwide for their therapeutic activities. However, the nature of interaction of β -lg with these derivatives remains unexplored. Fluorescence quenching studies suggest a static quenching mechanism for both the compounds. The average distances of 7.28 nm and 7.33 nm have been determined for IOC and PY respectively for energy transfer based on FRET which have application in many biological and biophysical fields. Circular dichroism spectra (CD) and Fourier transform infrared spectroscopy (FTIR) have been utilized to analyze the influence on the secondary structure of the protein. Docking simulation reveals a possible mechanism for different quenching behaviours and modes of binding preferred by the two compounds. Our findings will be helpful in the design of the drugs and other biologically active molecules that bind more strongly to β -lg and have the ability to show FRET.

Received 29th September 2016
Accepted 17th November 2016

DOI: 10.1039/c6ra24275h

www.rsc.org/advances

1 Introduction

Curcumin, a yellow lipid-soluble phenolic β -diketone dietary spice of turmeric, is found in the powdered root of *Curcuma longa* and is well known as a food coloring agent.¹ The pharmacological attributes of curcumin, such as antimalarial,² antioxidative,³ anti-inflammatory,⁴ anti-angiogenic,⁵ anti-amyloid,⁶ anti-cancer,⁷ anti-microbial,⁸ wound healing,⁹ and protective activities have been undergoing thorough research during last few decades due to its nontoxicity and bio-compatibility.¹⁰ This non-steroidal phytochemical has a medicinal value for liver diseases (jaundice), indigestion, urinary track diseases, rheumatoid arthritis & insect bites.¹¹ The β -diketone moiety of curcumin is responsible for keto-enol tautomeric behaviour, exerted enolic -OH (hydroxyl) group, and its instability *in vitro* as well as *in vivo*.¹² Anand *et al.* reported that the presence of β diketone moiety may play the crucial role in bio-activities but recent studies also show that the bioactivity of curcumin derivatives without β -diketones also revolved.¹³

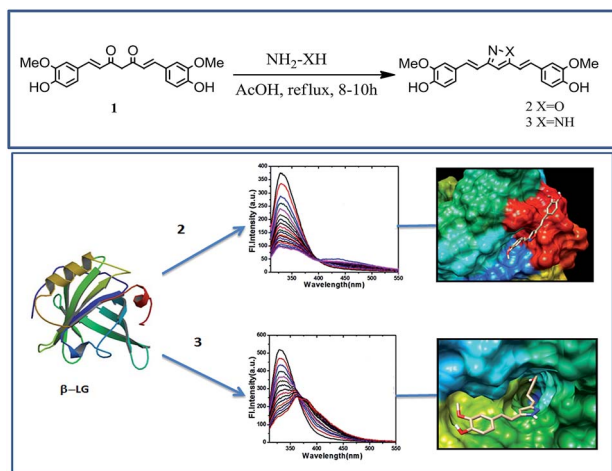
The pyrazole derivatives of curcumin has been deployed to study lipoxygenase inhibitory activity,¹⁴ endothelial cell proliferation and cytotoxicity.¹² Pyrazole and isoxazole derivatives also

maintain the binding to the sub domain of PKCs, protein kinase c6.¹⁵ Chakraborti *et al.* showed that both these derivatives were equally competent of binding to tubulin and resisting the tubulin self-assembly formation.¹⁶ The proposal for using these derivatives as an anti-cancer drug also had been under consideration due to their enhanced stability and free radical scavenging property.¹⁷ Nonetheless, pyrazole (PY) & isoxazole (IOC) derivatives are used as a potent ligand of fibrillar A β -42 aggregates.¹⁸ Various attempts have been made to increase the bioavailability and solubility of curcumin and its analogs either by nano capping or by nano encapsulation to various biological macromolecules.¹⁹ Bovine β -lg, a protein with hydrophobic core which consist with eight antiparallel β -strands called β -barrel or calyx, is one of the mostly used accepted carrier protein for hydrophobic ligands, having pH dependant opening, encapsulating property and a unique acidic pH resistivity.²⁰ In this way, bovine beta lactoglobulin (β -lg) performs the well-controlled drug delivery mechanism indeed.²¹ This encourages us to choose β -lg as a model carrier protein. Moreover, R. Narlawar *et al.* reported that curcumin derived isoxazoles and pyrazoles inhibit or modulate APP metabolism by interfering with γ -secretase activity.¹⁸

In order to go to mechanistic insight, our present work aims to study the interaction between these derivatives and the model protein β -lg utilizing different spectroscopic techniques (Scheme 1). These synthesized IOC and PY derivatives (shown in Scheme 1) exhibit excellent efficiency of energy transfer (FRET) from the Trp moiety (W_{19}) of β -lg in bound condition which will

Organic Chemistry Section, Department of Chemistry, Jadavpur University, Kolkata 700032, India. E-mail: uhalder2002@yahoo.com; Fax: +91 33 2413 7902; Tel: +91 33 2414 6223

† Electronic supplementary information (ESI) available. See DOI: 10.1039/c6ra24275h



Scheme 1 The synthesis of IOC and PY derivatives and their respective interaction with β -lg.

be a beneficial and staple technique for structural elucidation of biological molecules and their interactions *in vitro* assays, *in vivo* monitoring in cellular research, nucleic acid analysis, signal transduction, light harvesting and metallic nanomaterial.²² The conformational aspects of β -lg were also investigated through CD and FTIR studies. The modes of binding and encapsulation were also investigated through molecular docking method.

2 Results and discussion

2.1 UV-visible spectroscopy

Curcumin consists of a 1,3-diketone moiety that enables an extended conjugation of the π electron system between the two feruloyl groups.²³ The extended conjugation between two feruloyl moieties was disrupted due to lack of planarity by incorporation of isoxazole and pyrazole ring and the absorption maxima of these derivatives shifted at 335 and 325 nm respectively.²⁴ In these cases the λ_{\max} also shifts to the near UV region. Fig. 1(A) and (B) show the absorption spectra of IOC and PY derivatives in the absence and presence of varying concentrations of β -lg. The absorption spectrum of IOC and PY derivative show a prominent peak at 335 nm and 325 nm respectively and a weak shoulder at 291 nm for IOC and 298 nm for PY derivative respectively. These peaks appear due to n to π^* and π to π^* transitions in the IOC and PY derivatives of curcumin.

The forbidden n to π^* transition occurs in the high-energy ultraviolet region of the spectrum (291 nm for IOC and 298 nm for PY), while the π to π^* transitions occur in the lower energy end of the spectrum (335 nm for IOC and 325 nm for PY derivative). The intensity of the absorption bands at 335 and 291 nm for IOC and at 325 and 298 nm for PY gradually decreases on successive addition of protein, and the isosbestic points were observed at 303 nm for IOC and at 304 nm for PY. The formation of isosbestic point confirms the existence of interactions between IOC and PY derivative and β -lg and both the interacting species exist in equilibrium with one another at

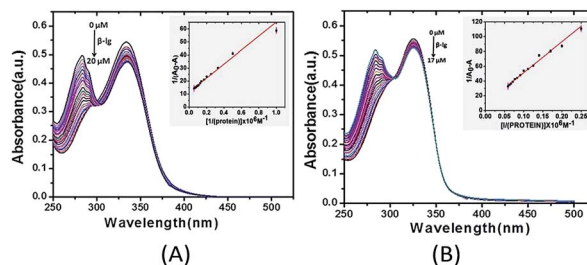


Fig. 1 UV-visible spectral changes of IOC (20 μ M) (A) and PY (20 μ M) (B) with the gradual addition of β -lg (1–20 μ M) and (1–17 μ M) respectively. Double reciprocal plot for 20 μ M IOC and 1–20 μ M β -lg [(A) inset] and double reciprocal plot for 20 μ M PY and 1–17 μ M β -lg [(B) inset] as per eqn (1). Relative errors have been expressed along with the corresponding error bars of respective data points (± 0.02).

that particular wavelength. The intensity of the bands at 335 nm and 325 nm are indicative of a greater hydrophobic/nonpolar environment.²³ Addition of β -lg enhances the polarity due to its charged nature, which also may be the reason for the decreased intensity at 335 and 325 nm. When IOC (20 μ M) was used, a sharp peak at 335 nm, a shoulder at 291 nm, and a weak absorption band at 285 nm are visible in the absorption spectrum (for IOC) and when of PY (20 μ M) was used, a sharp peak at 325 nm, a shoulder at 298 nm, and a weak absorption band at 285 nm are visible in the absorption spectrum.

The intensity of the absorption maxima of IOC at 335 nm decreases, and the absorption peak at 285 nm increases, simultaneously with increasing protein concentration 1 μ M to 20 μ M (Fig. 1(A)). In case of PY, same type of change of absorption maxima was observed at 325 nm and 285 nm (Fig. 1(B)) with increasing protein concentration 1 μ M to 15 μ M. The association constant (K_a) can be calculated from the following equation

$$1/\Delta A = 1/(\epsilon_b - \epsilon_f)L_T + 1/(\epsilon_b - \epsilon_f)L_T K_a M \quad (1)$$

where ϵ is the molar extinction coefficient and the subscripts b, f, and T refers to the bound, free, and total ligand concentration; L refers to the ligands (IOC, PY) and M refers to the macromolecule (β -lg, 1 to 20 μ M or 1 to 15 μ M). The equilibrium constant can be calculated by measuring the absorbance at a fixed wavelength. A double-reciprocal plot is obtained by plotting $1/(A_0 - A)$ against $1/[\text{protein}]$ [Fig. 1(A) inset and Fig. 1(B) inset]. The ratio of intercept and the slope gives the K_a value, which is found to be $1.83 \times 10^5 \text{ M}^{-1}$ for β -lg–IOC and $2.83 \times 10^4 \text{ M}^{-1}$ for β -lg–PY (Table S1) (ESI[†]). These values are well in agreement with the K_a values reported for strong interactions.²⁵

2.2 Fluorescence measurements

Fluorescence measurement is a convenient approach to understand the interaction between ligands and proteins because the fluorophore is responsive to the polarity of its surrounding environment.²⁶ In general, fluorescence intensity enhances as this polarity reduces.

Fluorescence quenching measurement of protein has been widely used to explore the binding properties of small molecule

with protein in solution. At excitation wavelength of 280 nm, both tryptophan (Trp) and tyrosine (Tyr) residues show fluorescence emission, but at 295 nm, only the Trp residue show fluorescence emission.²⁶ Bovine β -lg contains two Trp residues in positions 19 and 61. Trp₁₉ is located at the bottom of calyx, a strong hydrophobic region, while Trp₆₁ is situated near the aperture of the barrel which compels this residue exposed to the hydrophilic environment.²⁷ On the other hand; Trp₆₁ has close proximity of Cys₆₆-Cys₁₆₀ disulphide bridge which is a strong quencher of the fluorescence. So the fluorescence of β -lg at excitation wavelength of 295 nm is solely contributed by Trp₁₉. Fig. 2(A) and (B) represents the change of fluorescence intensities of β -lg in the presence of IOC and PY derivatives with an excitation wavelength at 295 nm. The steady-state fluorescence quenching patterns can be explained with the Stern–Volmer equation

$$F_0/F = 1 + K_{sv}[Q] = 1 + k_q\tau_0[Q] \quad (2)$$

where F and F_0 corresponds to the fluorescence intensity of β -lg in the presence and absence of two ligands respectively, $[Q]$ is the concentration of the ligands (quencher) and K_{sv} represents the Stern–Volmer quenching constant. τ_0 is the lifetime of the fluorophore without quencher ($\tau_0 = 10^{-8}$ s).²⁸ k_q is the bimolecular quenching rate constant.

The plot of F_0/F against the concentration of IOC and PY derivative [Fig. 2(A) and (B) inset] predicts to find the Stern–Volmer quenching constant K_{sv} , which were found to be $1.4 \times 10^5 \text{ M}^{-1}$ for IOC and $1.3 \times 10^5 \text{ M}^{-1}$ for PY (Table S1) (ESI†). Fluorescence quenching can be either static or dynamic. Static quenching arises when there is a complex formation between the fluorophore and the quencher in the ground state. The numbers of the fluorophore locating in the excited state thus were diminished. Hence, the fluorescence intensity is reduced in the presence of quencher. Dynamic or collision quenching occurs when the interaction between the fluorophore and the quencher appears in the excited state. The fundamental difference between the static and dynamic quenching lies in the

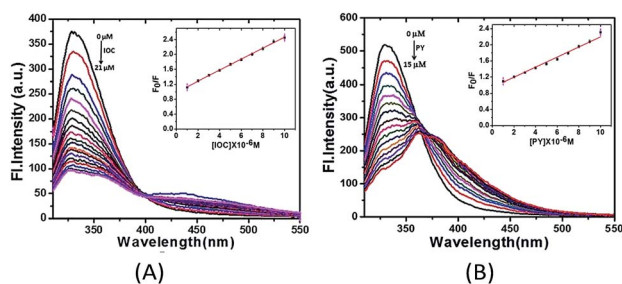


Fig. 2 (A) Fluorescence emission spectrum of β -lg (10 μM) in the absence and presence of IOC (1–21 μM). (B) Fluorescence emission spectrum of β -lg (10 μM) in the absence and presence of PY (1–15 μM). Inset: (A) plot of F_0/F versus $[\text{IOC}]$ and (B) plot of F_0/F versus $[\text{PY}]$ as per Stern–Volmer eqn (2). Excitations were done at 295 nm and emissions were observed at 329 nm for both IOC and PY derivatives. Slit width was 3 for excitation and 5 for emission for both the compounds. Relative errors have been expressed along with the corresponding error bars of respective data points (± 0.02).

lifetime of the fluorophore (10^{-8} s), for different concentrations of the quencher, which remains unchanged during static quenching (interaction takes place only in the ground state).²⁹

For dynamic quenching the following relation can be used

$$K_{sv} = k_q\tau_0 \quad (3)$$

where K_{sv} is Stern–Volmer quenching constant, k_q is the bimolecular quenching constant and τ_0 lifetime of the fluorophore (10^{-8} s).

The values of k_q of IOC and PY derivatives are $1.4 \times 10^{13} \text{ M}^{-1} \text{ S}^{-1}$ and $1.3 \times 10^{13} \text{ M}^{-1} \text{ S}^{-1}$ respectively (Table S1) (ESI†) and their k_q values are much higher than the maximum dynamic quenching constant ($2.0 \times 10^{10} \text{ M}^{-1} \text{ S}^{-1}$) in aqueous medium.^{26,29} Thus the result clearly shows that quenching is not due to collision factors but rather as a result of association between the fluorophore and the quencher in the ground state. So, in our case, mechanism of quenching is static in nature.

For the static quenching, the binding constant (K_s) and the binding sites (n) can be calculated employing the following equation

$$\log[(F_0 - F)/F] = \log K_s + n \log[Q] \quad (4)$$

where F_0 , F and $[Q]$ are the same as the parameters involved in Stern–Volmer equation. The linear plot of $\log[(F_0 - F)/F]$ as a function of $\log[\text{IOC}]$ and $\log[\text{PY}]$ are shown in Fig. 3(A) and (C). From the slope and intercept of the plot, the values of n (number of binding sites) and K_s can be obtained, which were shown in the Table S1.† The values of n are about 1 for both the IOC and PY derivatives. Thus it can be assumed that IOC– β -lg and PY– β -lg complexes were formed by the combination of one molecule of protein with one molecule of IOC and PY derivative separately.

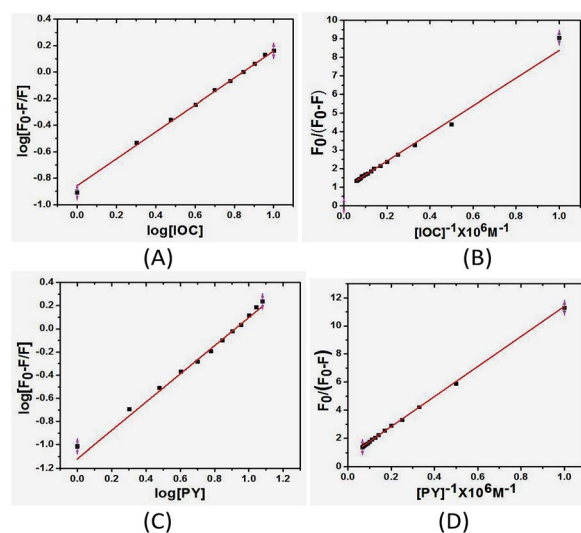


Fig. 3 (A) Plots of $\log[(F_0 - F)/F]$ vs. $\log[\text{IOC}]$ and (C) plots of $\log[(F_0 - F)/F]$ vs. $\log[\text{PY}]$ as per eqn (4). (B) Plots of $F_0/(F_0 - F)$ vs. $[\text{IOC}]^{-1} \times 10^6 \text{ M}^{-1}$ and (D) plots of $F_0/(F_0 - F)$ vs. $[\text{PY}]^{-1} \times 10^6 \text{ M}^{-1}$ as per modified Stern–Volmer eqn (5). Relative errors have been expressed along with the corresponding error bars of respective data points (± 0.02).

In addition, analogous results were observed by some workers studying interactions of other phenolic compound with β -lg or other proteins. For the interaction of β -lg with resveratrol the values of k_q and n were $3.6 \times 10^{13} \text{ M}^{-1} \text{ s}^{-1}$ and 1.2.²⁶ It also demonstrated that one molecule of β -lg combined with one molecule of resveratrol to form 1 : 1 complex and the mechanism of quenching is static.

The quenching constant K_a and the number of accessible fluorophore can be quantitatively determined following a modified Stern-Volmer equation,

$$F_0/(F_0 - F) = 1/f_a K_a Q + 1/f_a \quad (5)$$

where F_0 and F denote the fluorescence intensities in the absence and presence of two ligands respectively. K_a and f_a denote the quenching constant and the fraction of accessible fluorophore respectively. From the modified Stern-Volmer equation, plots of $F_0/F_0 - F$ against $1/[\text{ligand}]$ were shown for IOC and PY [Fig. 3(B) and (D)]. The quenching constant K_a was calculated from the ratio of the intercept to the slope, and the fraction of the accessible fluorophore (f_a) was calculated from the inverse of the intercept, which were found to be $1.04 \times 10^5 \text{ M}^{-1}$ and 1.203 for IOC and $6.83 \times 10^4 \text{ M}^{-1}$ and 1.39 for PY. The linearity of the plot depicts that both the ligands bind with β -lg to form 1 : 1 complexes.²⁷

In our study, steady state fluorescence data shows a sharp peak of IOC-derivative and PY-derivative at 437 nm and 391 nm upon excitation of the fluorophore at 335 nm and 325 nm maintaining the concentration at 10 μM for IOC and PY derivative respectively [Fig. 4(A) and (B)]. There was a gradual increase in fluorescence intensity of IOC derivative upon concomitant addition of β -lg solution up to 20 μM accompanied by a distinct blue shift in emission maxima about 17–20 nm. It signifies the encapsulation of IOC derivative into a more non polar microenvironment in presence of β -lg [Fig. 4(A)]. On the other hand, the increase in emission maxima in case of PY derivative was also observed without any significant change in emission maxima and was merely a blue shift of 6–8 nm [Fig. 4(B)], which signifies the accessibility of less hydrophobic environment as compared to the IOC derivative. This may indicate the different binding sites as well as the alteration in β -lg tertiary structure in presence of extrinsic fluorophore.

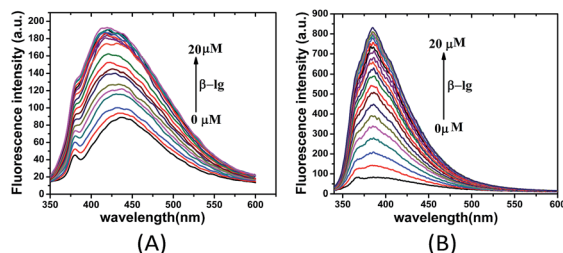


Fig. 4 (A) Fluorescence emission spectrum of IOC (10 μM) in the absence and presence of β -lg (1–20 μM). (B) Fluorescence emission spectrum of PY (10 μM) in the absence and presence of β -lg (1–20 μM). Excitations were done at 335 nm (IOC) and 325 nm (PY) and emissions were observed at 437 nm (IOC) and 391 nm (PY) respectively. Slit width was 3 for excitation and 5 for emission for both of the compounds.

2.3. Fluorescence resonance energy transfer (FRET)

FRET is an electrodynamic phenomenon that happens between a donor molecule in the excited state and an acceptor molecule in the ground state.³⁰ FRET study was considered to be an important parameter for study of energy transfer efficiency in between the donor and acceptor moiety, here β -lg acts as a donor and derivatives act as acceptors accordingly. The distance between ligands and Trp moieties in protein can be achieved by this method. In both the cases the FRET pattern shows the concomitant decrease in fluorescence intensity of Trp (W_{19}) in β -lg with gradual addition of IOC and PY derivatives accompanied by an increase in emission of extrinsic fluorophore ligands at their characteristic emission region, which signifies the efficient transfer of excited electronic energy from the donor site to the acceptor site [Fig. 2(A) and (B)]. According to the Förster's theory, the efficiency of the energy transfer, E , is established with the help of the following equations

$$E = 1 - F/F_0 = R_0^6/(R_0^6 + r^6) \quad (6)$$

where, F_0 and F are the fluorescence intensities in the absence and presence of equimolar amounts of ligands respectively, r is the distance from the ligands bound on β -lg to the Trp residue, and R_0 is the Förster's critical distance which can be defined as the distance at which 50% fluorescence energy transfer is possible from the donor site to the acceptor and was expressed as

$$R_0^6 = [8.79 \times 10^{-25} \times K^2 N^{-4} \Phi J] \quad (7)$$

here, the K^2 is a factor narrating the relative orientation in space for the transition dipoles of the donor and acceptor. K^2 is usually assumed to be equal to 2/3.³¹ N is the refractive index which is typically assumed to be 1.33 for bio molecules in aqueous solution. Φ is the quantum yield of the donor in the absence of acceptor and was considered to be 0.45.³² J is the overlap integral between the normalized emission spectra of the donor and absorption spectra of the acceptor. J is expressed by the following equation

$$J = \sum F(\lambda) \epsilon(\lambda) \lambda^4 d\lambda / \sum F(\lambda) d\lambda \quad (8)$$

In this equation, $F(\lambda)$ is the fluorescence intensity of the donor at wavelength λ and is dimensionless. $\epsilon(\lambda)$ is the molar absorption coefficient of the acceptor at wavelength λ . In the UV-absorption study, the concentrations of IOC and PY derivatives and the concentration of β -lg in fluorescence study kept constant [Fig. 5(A) and (B)]. J values calculated by integrating the overlap area of the spectra from 305 to 455 nm and were found to be $5.0046 \times 10^{-12} \text{ M}^{-1} \text{ cm}^3$ IOC and $3.7497 \times 10^{-12} \text{ M}^{-1} \text{ cm}^3$ for PY. The efficiency of energy transfer and Förster distance can be calculated from the eqn (6) and (7). Using the calculated value of R_0 and E , the value for r can be obtained. The R_0 values of IOC and PY derivatives were 8.66 nm and 8.25 nm respectively. The E values for IOC and PY derivatives were 0.74 and 0.51 respectively. The calculated r value is the average distance between ligand and two tryptophan residues (W_{19} and

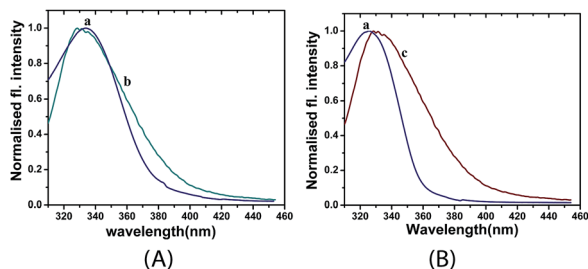


Fig. 5 (A) Spectral overlap of absorption spectra of IOC (b) and fluorescence spectra of β -lg (a). (B) Spectral overlap of absorption spectra of PY (c) and fluorescence spectra of β -lg (a). $c(\beta\text{-lg}) = c(\text{IOC}) = c(\text{PY}) = 1 \times 10^{-5} \text{ mol L}^{-1}$.

W_{61}) of β -lg. The r values were 7.28 nm for IOC and 7.33 nm for PY. The donor-to-acceptor distance lies within the range of $0.5R_0$ to $2R_0$ in each case, suggesting efficient energy transfer from β -lg to both of the ligands.³³ This suggests that one or both Trp residues are in close proximity to IOC and PY derivatives.

Bovine β -lg contains three binding sites, which are situated at the calyx, at the surface cleft and at the monomer/monomer interface.³⁴ The interactions of IOC and PY derivatives with β -lg are dominated by hydrophobic interaction as shown by FTIR study.

2.4. Time-correlated single-photon counting (TCSPC) study

We also extended our study for better understanding of steady state fluorescence results to time resolved fluorescence experiment by using SDS as prompt. The bi-exponential curve fitting programme, ran into the decay profiles, shows that the average life time, $\langle t \rangle$ of Trp in β -lg is 1.41 ns. Whereas, in presence of IOC, $\langle t \rangle$ of Trp is 1.38 ns and in presence of PY, $\langle t \rangle$ of Trp is 0.967 ns, this signifies that Trp was facing rather more polar environment in presence of IOC and PY at a higher extent resulting in decrease of average life time of Trp₁₉, and showing in Table 1 accompanied by the decrease in both longer and shorter life time components of Trp₁₉ present in the β -lg molecule. Nonetheless, the intrinsic time resolved fluorescence data shows decrease in average life time parameters, either cause by the change in micro polarity or by the change in micro conformation [Fig. 6(A)]. It also enlightens that the change is more pronounced in case of PY derivative than the IOC derivative. On the basis of this study it may be inferred that the micro polarity of the intrinsic fluorophore changed due to introduction of IOC

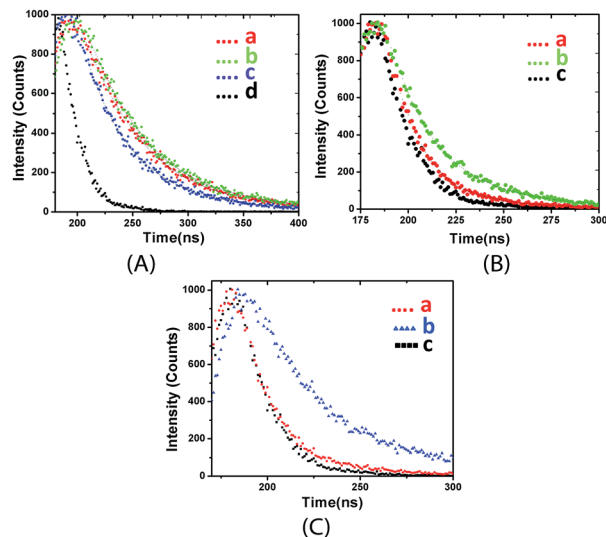


Fig. 6 (A) Time resolved fluorescence intensity decay profile of (a) Trp of native β -lg; (b) Trp in β -lg–IOC complex (1 : 1), (c) Trp in β -lg–PY complex (1 : 1) and (d) the sharp profile on the left (black) signifies for prompt. Excitation wavelength was chosen as 300 nm and fluorescence was collected at 350 nm. (B) Time resolved fluorescence intensity decay profile of (a) free IOC, (b) IOC in presence of β -lg (1 : 1) and (c) the sharp profile on the left (black) signifies for prompt. Excitation wavelength was chosen as 300 nm and fluorescence was collected at 410 nm. (C) Time resolved fluorescence intensity decay profile of (a) free PY, (b) in presence of β -lg (1 : 1), (c) the sharp profile on the left (black) signifies for prompt. Excitation wavelength was chosen as 300 nm and fluorescence was collected at 410 nm.

or PY and thus causing the change in micro-heterogeneity either by more solvent accessibility towards Trp moiety or due to proximity of substantial quencher moieties present in β -lg structure due to allostereism.

The extrinsic TCSPC fluorescence study shows that increase in average lifetime of both IOC and PY in presence of β -lg, which was accompanied by both the increase in longer and shorter lifetime parameters under bi exponential curve fitting programme, [Fig. 6(B) and (C)] it strongly signifies the anchoring of the IOC and or PY to a less polar or more hydrophobic micro environment in β -lg matrix (Table 1) either they found the hydrophobic pockets of β -lg or they get confined into more hydrophobic regions within the β -lg matrix under altered conformation. The relative confinements of the derivatives are more pronounced in case of PY, which depicts the better binding of PY, in β -lg hydrophobic calyx. It may also be

Table 1 Time-correlated single-photon counting (TCSPC) parameters

Compounds	a_1	τ_1 (ns)	a_2	τ_2 (ns)	χ^2	τ_{av} (ns)
Trp in native β -lg	0.925	1.28	0.074	3.06	0.9432	1.41
Trp in IOC + β -lg (1 : 1)	0.69	1.05	0.309	2.14	1.0263	1.38
Trp in PY + β -lg (1 : 1)	0.67	0.67	0.33	1.57	1.0494	0.967
IOC (free)	0.971	0.15	0.028	1.005	1.0881	0.173
IOC in presence of β -lg	0.942	0.241	0.0577	1.132	1.0838	0.3
PY (free)	0.250	0.142	0.025	0.991	1.0656	0.163
PY in presence of β -lg	0.766	0.498	0.2339	1.709	1.0129	0.781

proposed that the presence of more hydrophobic aromatic moieties enhances the binding with PY, either by π - π type of interactions or by H-bonding, which has been thoroughly studied in docking experiment.

2.5. CD results

The change in secondary structure of β -lg in presence of ligands was investigated by circular dichroism spectroscopy (CD). Far UV-CD spectra analysis shows insignificant change in the minima at 215 nm, characteristic β -sheet signal for β -lg structure.³⁵ It clearly shows that the secondary structure of β -lg remains almost intact during binding with IOC [Fig. 7(A)]. In the presence of PY, a distinctive change of β -lg conformation occurs, resulting from the enhanced signals at 208 and 222 nm and thus indicating more α -helical structure upon binding with β -lg [Fig. 7(B)]. It clearly indicates an evidence of allosterism in β -lg conformation when it binds with PY derivative. The appearance of a strong signal at 208 nm at higher concentration of PY derivative primarily indicates the cumulative change arising from the alteration of tertiary structure and hence the change in micro environment and it was also supported by steady state fluorescence study. The calculation of secondary structural changes of β -lg in presence of IOC and PY derivative was done by CDNN software and shown in Table S3 (ESI[†]).

2.6. FT-IR spectra

Infrared (IR) spectroscopy is one of the well-established experimental techniques for the analysis of secondary structure of proteins. The vibrations of a protein structure give rise to nine characteristic IR absorption bands, namely, amide A, B, and

I–VII. Of these, the amide I and II bands are the most important bands. They are sensitive to the protein secondary structure. The amide-I peak position occurs in the region of 1700–1600 cm^{-1} (mainly C=O stretch), amide-II band in the region of 1600–1500 cm^{-1} (C–N stretch coupled with N–H bending mode). Amide I band is useful and more sensitive to the change of protein secondary structure than amide II band.³⁶ In our study amide I band was monitored to investigate the change of secondary structure of β -lg in the presence and absence of the ligands IOC and PY. Native β -lg molecule in absence of any derivatives shows the amide-I band at around 1632 cm^{-1} which is the characteristic feature for the globular protein like β -lg having predominant β -sheet structure [Fig. 7(C) spectra a].³⁷ Thus the shifting of amide-I band of native β -lg occurs from 1632 cm^{-1} to 1650 cm^{-1} (bathochromic shift) in presence of two derivatives. Our experimental results clearly indicate a sharp secondary structural transition of β -lg from predominant β -sheet structure to α -helical structural contents upon binding with IOC and PY derivatives. Furthermore, the PY derivative is more effective than IOC derivative to incorporate such structural transition during their binding with β -lg. These observations were noted during the study of far UV-CD spectra.

2.7. Docking study

The protein β -lg is a small globular protein with the molecular mass 18 400 Da. There are 162 amino acid residues constructing eight antiparallel β -strands forming the β -barrel or calyx, and one α -helix at the outer surface of the barrel in the monomeric form of β -lg. Three binding pockets for ligands: the calyx, a small space between α -helix and the barrel and the region near Trp₁₉–Arg₁₂₄, are found in the tertiary structure of β -lg. Between the two tryptophan residues, Trp₆₁ and Trp₁₉, the Trp₁₉ of the protein is mainly responsible for its fluorescence nature. If a fluorophore bind with the protein in such a way that it comes into the Förster distance of any of the Trp residues, then that Trp residue can transfer its energy efficiently to the fluorophore after excitation. The phenomenon is popularly known as FRET.

The molecular docking study has drawn much attention to both the theoretical and experimental researchers. It is frequently used to determine the binding behavior of small molecules into the target specific protein environment where they bind mainly through a non-covalent interaction like hydrogen bonding, electrostatic and steric effects, van der Waal's forces and stacking interactions. A molecular docking study has been carried out with IOC and PY on β -lg (PDB ID: 3NQ3) to find protein environment where they interact. The energetically most favourable docking positions were calculated. It has been observed that both the molecule stabilized into the binding site through hydrogen bonding, π -stacking, π -alkyl, π -anion and π -sigma interaction. The change of Gibbs free energy has been calculated for IOC and PY and was found to be -5.45 and -6.55 kcal mol⁻¹ respectively. This result indicates that PY binds with β -lg more strongly than that of IOC. The compound IOC prefers surface binding at the region near Trp₁₉–Arg₁₂₄ through H-bonding with Trp₁₉ and Tyr₂₀, π -stacking with Tyr₂₀ and other π -interaction with Glu₄₄ and Glu₁₅₈ [Fig. 8(A)–(C)]. However, PY binds inside the calyx [Fig. 9(A) and (B)] and

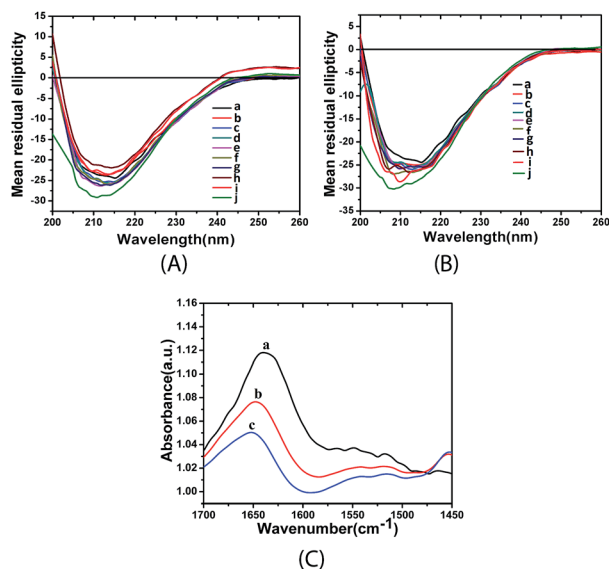


Fig. 7 (A) CD spectra of (a) β -lg (13.6 μM) in the presence of (b) 5 μM , (c) 10 μM , (d) 15 μM , (e) 20 μM , (f) 30 μM , (g) 40 μM , (h) 50 μM , (i) 100 μM , (j) 200 μM IOC. (B) CD spectra of (a) β -lg (13.6 μM) in the presence of (b) 5 μM , (c) 10 μM , (d) 15 μM , (e) 20 μM , (f) 30 μM , (g) 40 μM , (h) 50 μM , (i) 100 μM , (j) 200 μM PY. (C) FTIR spectra of (a) free β -lg (500 μM), (b) complex of β -lg with IOC (1 : 1) and (c) complex of β -lg with PY (1 : 1).

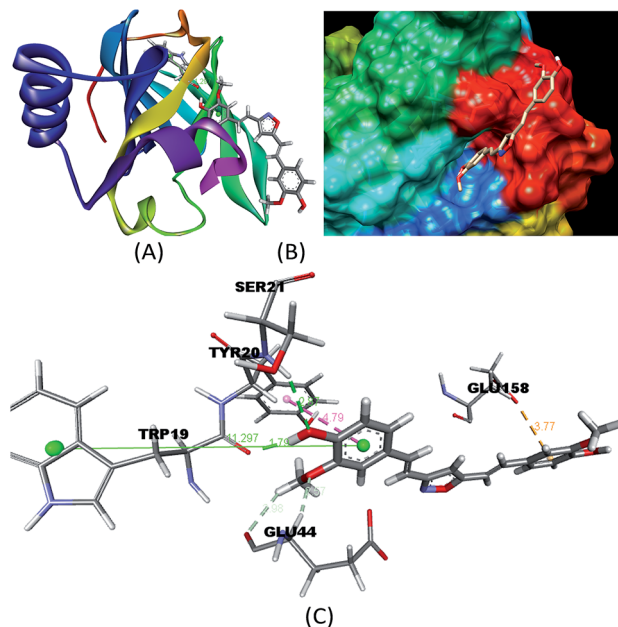


Fig. 8 Schematic representation of docked conformation of IOC with interacting residues of β -lg. Docking pose shows IOC binds at the surface of the protein.

Val₄₃, Ile₅₆, Ile₈₄, Asn₉₀, Val₉₂, Phe₁₀₅, Met₁₀₇ and Asn₁₀₉, residues of the protein are in the vicinity of the molecule [Fig. 9(C)]. In this environment of the protein, PY molecule is stabilized by H-bonding with Asn₁₀₉, π -stacking with Phe₁₀₅ and other π -interaction with Asn₉₀, Ile₈₄, Ile₅₆, Val₄₃, Val₉₂ and Met₁₀₇ residues.

Docking results also shows that IOC and PY are inside the region of the Förster distance of Trp₁₉ and Trp₆₁ respectively. The distance between compound IOC and Trp₁₉ is 11.3 Å which

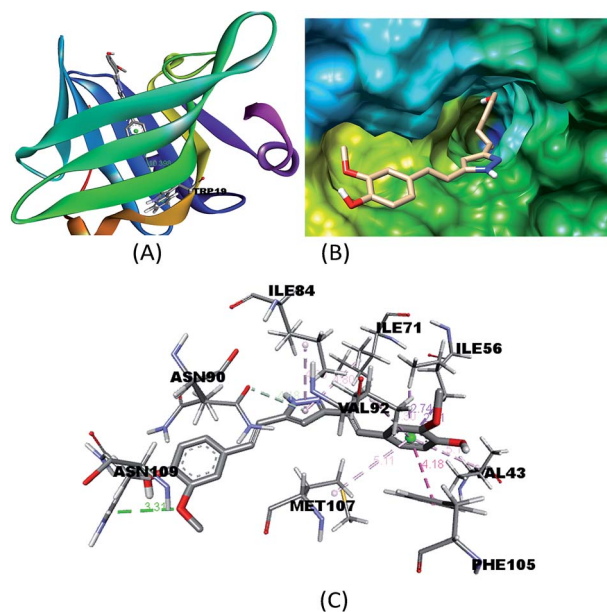


Fig. 9 Schematic representation of docked conformation of PY with interacting residues of β -lg. Docking pose shows PY binds inside the calyx of the protein.

is under the range of Förster distance (range of $0.5R_0$ to $2R_0$, experimentally determined R_0 value is 8.66 Å, so the range become 4.33 Å to 17.32 Å). However, in the case of compound PY the Trp₆₁ is 10.4 Å apart from it. This is also under the Förster distance range of Trp₆₁ (for this compound experimentally determined R_0 value is 8.25 Å and the range is 4.12 Å to 16.50 Å). Docking study successfully predict the ability to show FRET with β -lg for both the compound.

3 Experimental

3.1. Materials and methods

Bovine β -lactoglobulin (β -lg) was isolated and purified from cow milk described earlier.³⁸ Pure curcumin was purchased from Sigma-Aldrich, India. IOC and PY were synthesized according to the methods.³⁹ IOC and PY were further characterised by ¹H-NMR, ¹³C-NMR and ESI-MS (all spectra and data were given in the ESI†). Protein stock solutions were prepared using phosphate buffer containing 2% ethanol pH-7.4 while IOC and PY stock solutions prepared in absolute ethanol because of its poor solubility in aqueous buffer. Concentrations of IOC, PY and β -lg were determined spectroscopically using extinction co-efficient of β -lg $0.96 \text{ mg}^{-1} \text{ ml}^{-1} \text{ cm}^{-1}$ at 280 nm and molar extinction coefficient $40\,268 \text{ M}^{-1} \text{ cm}^{-1}$ at 335 nm for IOC and $42\,246 \text{ M}^{-1} \text{ cm}^{-1}$ at 325 nm for PY.²⁴

3.2. Instrumentation

3.2.1. UV-visible spectroscopy. Absorbance measurements for the determination of binding affinity and binding constants were performed utilizing UV-Visible SHIMADZU Spectrophotometer model no. TCC-240A at room temperature (25 °C). UV titrations were performed in a 1 cm quartz cuvette with the concentration of IOC (20 μM) and PY (20 μM) as constant and by the successive addition of increasing concentrations of β -lg (1–20 μM) for IOC and (1–17 μM) for PY. The respective spectra were recorded over the wavelength range 200–600 nm.

3.2.2. Spectrofluorimetry. Fluorescence quenching studies were carried out using Shimadzu RF-5301 PC at room temperature with the bandwidths of excitation and emission slits at 3 and 5 nm respectively. Both the extrinsic fluorescence titration was performed, firstly keeping the ligand concentration fixed at 10 μM and varying protein concentration and *vice versa*. The concentration of β -lg (10 μM) was kept constant and then IOC and PY added successively from 1 to 21 μM and 1 to 15 μM . The excitation wave length was 335 nm and 325 nm for IOC and PY derivative and emission was recorded from 350–550 nm. For FRET study purpose, the excitation wavelength of β -lg (10 μM , with phosphate buffer, pH-7.4, with 2% ethanol) was 295 nm and emission scans were recorded in the range 310–550 nm at room temperature.

3.2.3. Time resolved fluorescence study. Lifetime measurements were acquired using the time-correlated single-photon counting (TCSPC) apparatus using a picoseconds diode laser at 295 nm (IBH, UK, nanoLED-295) as the light source and TBX-04 as detector. The full width at half-maximum (FWHM) of the instrument response function was 1 ns. All the

measurements were done in a 45 ns time window with a resolution of 100 ps per channel. A 1 cm path length quartz cuvette was used for all the time-resolved measurements. Fluorescence decays were collected at the magic angle (polarization of 54.7°) with respect to the vertical excitation light at 295 nm. Excitation at 295 nm exclusively for tryptophan residues and prevent background fluorescence from other aromatic amino acids like phenyl alanine and tyrosine. In another experiment beta lactoglobulin mixed with IOC and PY derivative of curcumin with 1 : 1 molar ratio. In both cases the excitation wavelength was 300 nm and life time decay traces were obtained from 400 to 450 nm. The decays were analyzed using IBH DAS-6 decay analysis software.

3.2.4. CD spectroscopy. CD spectra of β -lg and IOC and PY derivative of curcumin complexes were recorded on a Jasco spectropolarimeter (J-815). For measurements in the far-UV (200–260 nm) region, quartz cell in the path length 0.2 cm was used in the nitrogen atmosphere. Concentration of β lg was kept constant (13.6 μ M) while varying concentrations (5 μ M, 10 μ M, 15 μ M, 20 μ M, 30 μ M, 40 μ M, 50 μ M, 100 μ M, 200 μ M) of IOC and PY derivatives. Scan speed 50 nm per minute was performed and data were collected for each nm from 260 to 200 nm. Sample temperature was maintained at 25 °C using a Neslab RTE-111 circulating water bath connected to the water jacketed quartz cuvettes. The secondary structures of β -lg were calculated from CDNN 2.1 software.

3.2.5. FT-IR absorption spectra. The infra-red absorption spectra of the compounds and β -lg solution were measured at room temperature. FT-IR scans were recorded in the range of 1550–1750 cm^{-1} at a resolution of 2 cm^{-1} in N_2 environment using a Spectrum 100 FT-IR spectrometer (Perkin Elmer) with ATR accessory. The concentration of β -lg was 500 μ M.

3.2.6. Molecular modeling study. The crystal structure of β -lg was obtained from RCSB Protein Data Bank website (PDB ID: 3NQ3), the structure of the biopolymer was analysed and prepared for the docking experiment. The structure of IOC and PY were optimized to lower energy using Density Functional Theory (DFT) B3LYP/6-31G level of theory. These optimized structures were used for docking with β -lg protein to find the probable site and mode of binding using a grid-based docking program Auto Dock 4.2. For the docking study, ligand present in the protein (3NQ3) and water molecules were removed from the protein, atom Kollman charges were assigned after the addition of polar hydrogen for the protein. The default parameters of Auto Dock and generic algorithm were used for this calculation. The visualization effects were prepared by Discovery Studio 4.1 Client and Chimera 1.10.1rc.

4 Conclusion

In this work, the interactions between β -lg and curcumin derivatives follow static quenching mechanism which was established through fluorescence quenching experiments. IOC and PY can interact with β -lg to form 1 : 1 complexes, without apparent effects on the secondary structure of protein while binding with IOC but significant conformational changes of protein were observed while binding with PY. Both IOC and PY

remain inside the region of the Förster distance of Trp₁₉ and Trp₆₁ of β -lg to exhibit FRET as evidenced by docking experiment. The change in micro polarity as a result of the change in micro conformation was more pronounced in case of PY derivative than that of IOC derivative as revealed from time resolved fluorescence data. FTIR data also supports the conformational changes of β -lg with these compounds. The studies of interaction of IOC and PY with β -lg suggest an effective association with PY compared to IOC. The compound IOC favours surface binding at the region near Trp₁₉–Arg₁₂₄ through H-bonding and other weak forces. However, PY prefers to bind inside the calyx and stabilization was achieved by H-bonding with Asn₁₀₉, π -stacking with Phe₁₀₅ and other π -interaction with Asn₉₀, Ile₈₄, Ile₅₆, Val₄₃, Val₉₂ and Met₁₀₇ residues. This preliminary study and useful information about the interaction of curcumin derivatives furnishes the promise in designing the drugs and other biologically active molecules that bind more strongly to β -lg and have ability to show FRET.

Conflict of interest

The authors declare no competing financial interest.

Acknowledgements

Financial support of University Grant Commission UGC-CAS-II and DST-PURSE-II (Govt. of India) Program of Department of Chemistry, Jadavpur University, Kolkata are greatly acknowledged. Sanhita Maity, SRF, is a recipient of UGC-NET Research Fellowship in Chemistry.

References

- 1 J. S. Jurenka, *Alternative Med. Rev.*, 2009, **14**, 2.
- 2 R. C. Reddy, P. R. C. Reddy, P. G. Vatsala, V. G. Keshamouni, G. Padmanaban and P. N. Rangarajan, *Biochem. Biophys. Res. Commun.*, 2005, **326**, 472.
- 3 R. K. Maheshwari, A. K. Singh, J. Gaddipati and R. C. Srimal, *Life Sci.*, 2006, **78**, 2081.
- 4 N. C. Wu, *Journal of Alternative and Complementary Medicine*, 2003, **9**, 161.
- 5 P. Yoysungnoen, P. Wirachwong, C. Changtam, A. Suksamrarn and S. Patumraj, *World J. Gastroenterol.*, 2008, **14**, 2003.
- 6 J. M. Ringman, S. A. Frautschy, G. M. Cole, D. L. Masterman and J. L. Cummings, *Curr. Alzheimer Res.*, 2005, **2**, 131.
- 7 R. Wilken, M. S. Veena, M. B. Wang and E. S. Srivatsan, *Mol. Cancer*, 2011, **10**, 12.
- 8 P. Tyagi, M. Singh, H. Kumari, A. Kumari and K. Mukhopadhyay, *PLoS One*, 2015, **10**, e0121313.
- 9 D. Akbika, M. Ghadiria, W. Chrzanoskia and R. Rohanizadeh, *Life Sci.*, 2014, **116**, 1.
- 10 K. Sindhu, A. Rajaram, K. J. Sreeram and R. Rajaram, *RSC Adv.*, 2014, **4**, 1808.
- 11 A. Majhi, G. M. Rahman, S. Panchal and J. Das, *Bioorg. Med. Chem.*, 2010, **18**, 1591.

- 12 A. Vyas, P. Dandawate, S. Padhye, A. Ahmad and F. Sarkar, *Curr. Pharm. Des.*, 2013, **19**, 2047.
- 13 S. G. Anand, A. B. Thomas, K. C. Sundarama, K. B. Harikumara, B. Sunga, S. T. Tharakana, K. Misra, I. K. Priyadarsini, K. N. Rajasekharan and B. B. Aggarwala, *Biochem. Pharmacol.*, 2008, **76**, 1590.
- 14 A. Koeberle, E. Muñoz, G. B. Appendino, A. Minassi, S. Pace, A. Rossi, C. Weinigel, D. Barz, L. Sautebin, D. Caprioglio, J. A. Collado and O. Werz, *J. Med. Chem.*, 2014, **57**, 5638.
- 15 J. Das, S. Pany, S. Panchal, A. Majhi and G. M. Rahman, *Bioorg. Med. Chem.*, 2011, **19**, 6196.
- 16 S. Chakraborti, G. Dhar, V. Dwivedi, A. Das, A. Poddar, G. Chakraborti, G. Basu, P. Chakrabarti, A. Surolia and B. Bhattacharyya, *Biochemistry*, 2013, **52**, 7449.
- 17 A. Vyas, P. Dandawate, S. Padhye, A. Ahmad and F. Sarkar, *Curr. Pharm. Des.*, 2013, **19**, 2047.
- 18 R. Narlawar, M. Pickhardt, S. Leuchtenberger, K. Baumann, S. Krause, T. Dyrks, S. Weggen, E. Mandelkow and B. Schmidt, *ChemMedChem*, 2008, **3**, 165.
- 19 R. K. Gangwar, G. B. Tomar, V. A. Dhumale, S. Zinjarde, R. B. Sharma and S. Datar, *J. Agric. Food Chem.*, 2013, **61**, 9632.
- 20 Z. Teng, R. Xua and Q. Wang, *RSC Adv.*, 2015, **5**, 35138.
- 21 S. P. Bull, Y. Hong, V. V. Khutoryanskiy, J. K. Parker, M. Faka and L. Methven, *Food Quality and Preference*, 2017, **56**, 233.
- 22 S. A. Hussain, D. Dey, S. Chakraborty, J. Saha, A. D. Roy, S. Chakraborty, P. Debnath and D. Bhattacharjee, *Science Letters Journal*, 2015, **4**, 119.
- 23 P. Kumaraswamy, S. Sethuraman and U. M. Krishnan, *J. Agric. Food Chem.*, 2013, **61**, 3278.
- 24 B. K. Sahoo, K. S. Ghosh and S. Dasgupta, *Biophys. Chem.*, 2008, **132**, 81.
- 25 B. k. Sahoo, K. S. Ghosh and S. Dasgupta, *Protein Pept. Lett.*, 2009, **16**, 1485.
- 26 L. Liang, H. A. Tajmir-Riahi and M. Subirade, *Biomacromolecules*, 2008, **9**, 50.
- 27 B. J. Harvey, E. Bell and L. Brancaloni, *J. Phys. Chem. B*, 2007, **111**, 2610.
- 28 F. Mohammadi, A. K. Bordbar, A. Divsalar and A. A. Saboury, *Protein J.*, 2009, **28**, 117.
- 29 A. Sahu, N. Kasoju and U. Bora, *Biomacromolecules*, 2008, **9**, 2905.
- 30 J. R. Lakowicz, *Principles of fluorescence spectroscopy*, Springer, 2006, p. 443.
- 31 S. Chatterjee, S. Nandi and S. C. Bhattacharya, *J. Photochem. Photobiol., A*, 2005, **173**, 221.
- 32 P. Patrick, *Eur. J. Biochem.*, 1976, **63**, 263.
- 33 J. R. Lakowicz, *Principles of fluorescence spectroscopy*, Springer, 2006, p. 445.
- 34 G. Kontopidis, C. Holt and L. Sawyer, *J. Mol. Biol.*, 2002, **318**, 1043.
- 35 S. Sardar, S. Pal, S. Maity, J. Chakraborty and U. C. Halder, *Int. J. Biol. Macromol.*, 2014, **69**, 137.
- 36 L. Yongchun, Y. Zhengyin, D. Juan, X. Yao, L. Ruixia, Z. Xudong, L. Jianning, H. Huaisheng and L. Hong, *Immunobiology*, 2008, **213**, 651.
- 37 S. Maity, S. Sardar, S. Pal, H. Parvej, J. Chakraborty and U. C. Halder, *RSC Adv.*, 2016, **6**, 74409.
- 38 J. Chakraborty, N. Das, K. P. Das and U. C. Halder, *Int. Dairy J.*, 2009, **19**, 43.
- 39 M. W. Amolins, L. B. Peterson and B. S. Blagg, *Bioorg. Med. Chem.*, 2009, **17**, 360.